

CHNNet: An Artificial Neural Network With Connected Hidden Neurons

Rafiad Sadat Shahir Zayed Humayun
 Md. Golam Rabiul Alam

BRAC University

{rafiad.shahir, zayed.humayun, rabiul.alam, abu.khan}@bracu.ac.bd
 {mashrufa.akter.tamim, shouri.saha}@g.bracu.ac.bd

Mashrufa Akter Tamim Shouri Saha
 Abu Mohammad Khan

Abstract

In contrast to biological neural circuits, conventional artificial neural networks are commonly organized as strictly hierarchical architectures that exclude direct connections among neurons within the same layer. Consequently, information flow is primarily confined to feedforward and feedback pathways across layers, which limits lateral interactions and constrains the potential for intra-layer information integration. We introduce an artificial neural network featuring intra-layer connections among hidden neurons to overcome this limitation. Owing to the proposed method for facilitating intra-layer connections, the model is theoretically anticipated to achieve faster convergence compared to conventional feedforward neural networks. The experimental findings provide further validation of the theoretical analysis.

1. Introduction

Artificial Neural Networks (ANNs) are conceptualized as simplified computational models inspired by the organizational principles of biological neural systems. Empirical studies suggest that the human brain exhibits dense hierarchical and lateral connectivity patterns, which facilitates dynamic information exchange and adaptive processing [3, 4]. Such lateral interactions among neural populations play a crucial role in coordinating representations, minimizing redundancy, and enhancing the stability of learning processes. Early computational abstractions, such as the McCulloch–Pitts neuron [15], were inspired by biological principles but did not adequately represent the intricate connectivity patterns observed in real neural circuits.

As the field progressed, artificial neural architectures predominantly adopted a structured feedforward topology. In a typical Feedforward Neural Network (FNN), neurons in a given layer connect exclusively to neurons in adjacent layers, remaining independent of one another within the same layer. This design promotes computational efficiency and

stable gradient propagation, but diverges from the biological principle of lateral interactivity. Consequently, while such architectures are effective in hierarchical information processing, they lack internal communication mechanisms that can potentially enable richer and more adaptive representational learning.

Several recent studies have extended beyond conventional designs to incorporate increased connectivity among the neurons [1, 2, 5, 12, 13, 20, 21]. Nonetheless, the introduction of intra-layer connections among hidden neurons and their potential impact on the network’s learning dynamics remain largely unexplored.

In exploring this issue, we introduce an extended feedforward model in which neurons within the same hidden layer share information through learnable lateral connections. This structural modification maintains the feedforward architecture while introducing intra-layer communication reminiscent of cortical interactions in biological systems. We refer to this network as CHNNet, with the primary aim of investigating the functional consequences of introducing lateral connectivity absent in conventional architectures.

Collectively, we reconsider a fundamental architectural assumption of feedforward networks that neurons within the same layer operate in isolation and demonstrate that relaxing this constraint can lead to notable improvements in learning dynamics.

2. Theoretical Study

In this study, we analyze the proposed CHNNet architecture from the perspective of conventional FNNs, focusing on its modifications to the hidden layer connectivity and their impact on the learning behavior of the network.

2.1. Architecture

The architecture of CHNNet extends conventional FNN architectures by incorporating additional interconnections among hidden neurons, as illustrated in figure 1 with example networks containing one and two hidden layers. We

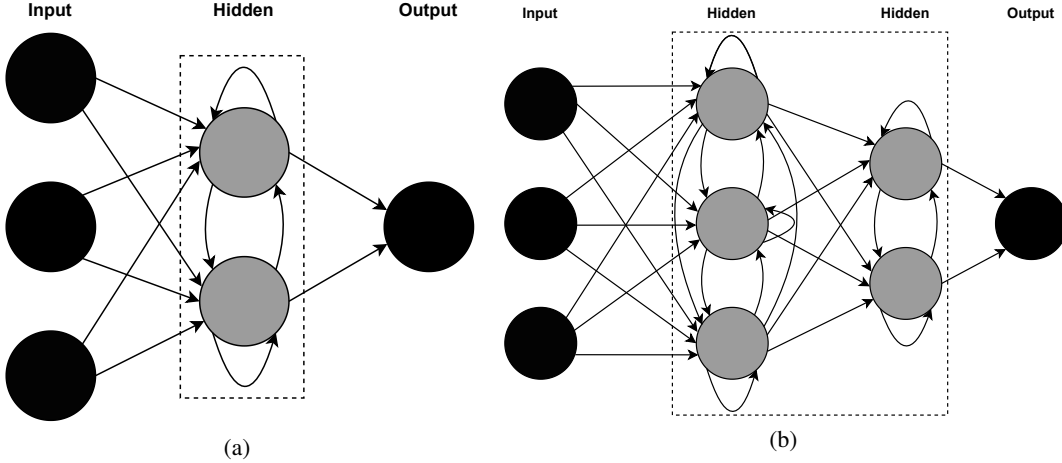


Figure 1. The architecture of CHNNet with (a) one hidden layer and (b) two hidden layers.

propose modifications exclusively to the connectivity of the hidden layers, while the input and output layers remain unaltered.

2.2. Inference Mechanism

We define the pre-activation output of a hidden layer in CHNNet, denoted by z , as follows:

$$z^{[l]} = W_1^{[l]} a^{[l-1]} + W_2^{[l]} h^{[l]} + b^{[l]} \quad (1)$$

Consider that a is the post-activation output of a hidden layer, h is the post-activation output of the hidden neurons of the current layer, W_1 is the weight matrix for the connections of the previous layer to the current layer, W_2 is the weight matrix for the intra-layer connections of the hidden layer, b is the bias vector and l denotes the index of the hidden layer.

The variable h in equation (1) is a distinctive component of CHNNet, differentiating it from conventional FNNs. We propose to compute h by applying the identity function f_I as follows:

$$\begin{aligned} h^{[l]} &= f_I(W_1^{[l]} a^{[l-1]} + b^{[l]}) \\ &= W_1^{[l]} a^{[l-1]} + b^{[l]} \end{aligned} \quad (2)$$

Subsequently, the post-activation output of the hidden layer is computed by applying the activation function f as follows:

$$a^{[l]} = f^{[l]}(z^{[l]}) \quad (3)$$

Since the connectivity of the output layer is unaltered, the post-activation output of the output layer for a network comprising L layers is computed as follows:

$$z^{[L]} = W_1^{[L]} a^{[L-1]} + b^{[L]} \quad (4)$$

$$a^{[L]} = f^{[L]}(z^{[L]}) \quad (5)$$

2.3. Comparison with Multilayer Perceptrons

In the foundational stages of neural network research, Minsky and Papert [16] introduced the conceptual basis of the Multilayer Perceptron (MLP), describing it as a hierarchical model without intra-layer connections among hidden neurons. Subsequently, Rumelhart et al. [19] conducted extensive analysis of various MLP architectures, none of which incorporated intra-layer connections. The pre-activation output in these studies is commonly formulated as follows:

$$z^{[l]} = W^{[l]} a^{[l-1]} + b^{[l]} \quad (6)$$

Equation (6) differs substantially from the corresponding CHNNet formulation in equation (1).

2.4. Comparison with Recurrent Neural Networks

Recurrent Neural Networks [19] introduced feedback loops that allow information to propagate through time, enabling temporal modeling of sequential data. The Hopfield Network [8] and the Boltzmann Machine [7] further extended connectivity by employing symmetric bidirectional links among neurons, functioning respectively as an associative memory model and a probabilistic representation learner.

Neural architectures such as the Echo State Network [10] and the Liquid State Machine [14] employ a reservoir of randomly connected neurons that provides nonlinear modeling capabilities.

Within Spiking Neural Networks (SNNs), intra-layer connections in the hidden layer have been proposed by Cheng et al. [2], Zhang et al. [21], and Chen et al. [1], while self-connections have been introduced by Zhang and Zhou [20].

Notably, each of the aforementioned studies incorporates some form of recurrent connectivity within the hidden neurons. In these studies, the pre-activation output at time step

t is generally formulated as follows:

$$z_t^{[l]} = W_1^{[l]} a_t^{[l-1]} + W_2^{[l]} h_{t-1}^{[l]} + b^{[l]} \quad (7)$$

Nevertheless, the intra-layer connections in CHNNNet differ fundamentally from recurrent connections. While RNNs compute the hidden layer output using activations from the previous time step, CHNNNet utilizes the linear activations of hidden neurons within the current time step, as shown in equation (1).

2.5. Comparison with Skip-Connections

Recent advances in neural network design have focused on creating new pathways for information flow. Convolutional Neural Network (CNN) architectures, including DenseNet [9], ResNet [5], UNet [18], and UNet++ [22], employ skip connections to propagate information directly from one layer to subsequent deeper layers.

Although the model's computations of inputs from hidden neurons are sometimes interpreted as forming two conventional FNN layers linked by a skip connection, the architecture in fact implements intra-layer coupling within a single layer rather than a stacked two-layer structure. To clarify this distinction, consider the following derivation based on equation (1):

$$\begin{aligned} z &= W_1 a + W_2 h + b \\ &= W_1 a + W_2 (W_1 a + b) + b \\ &= W' a + b' \end{aligned} \quad (8)$$

From equation (8), it follows that the hidden layers of CHNNNet operate effectively as a single layer, rather than as two distinct conventional FNN layers.

2.6. Learning Mechanism

In this study, we have analyzed CHNNNet exclusively using backpropagation as the learning mechanism. CHNNNet comprises three learnable parameters, specifically weights W_1 , W_2 , and bias b . Computing the gradients of these parameters is straightforward.

For the l^{th} layer in a conventional FNN, the partial derivative of the loss function, denoted as J , with respect to a learnable parameter W is computed as follows:

$$\frac{\partial J}{\partial W^{[l]}} = \frac{\partial J}{\partial z^{[l]}} \frac{\partial z^{[l]}}{\partial W^{[l]}} \quad (9)$$

For CHNNNet, the partial derivative of the loss function with respect to W_2 is computed as follows:

$$\frac{\partial J}{\partial W_2^{[l]}} = \frac{\partial J}{\partial z^{[l]}} \frac{\partial z^{[l]}}{\partial W_2^{[l]}} \quad (10)$$

Differing from conventional FNNs, the partial derivatives of the loss function with respect to W_1 and b are computed as follows:

$$\frac{\partial J}{\partial W_1^{[l]}} = \frac{\partial J}{\partial z^{[l]}} \left(\frac{\partial z^{[l]}}{\partial W_1^{[l]}} + \frac{\partial z^{[l]}}{\partial h^{[l]}} \frac{\partial h^{[l]}}{\partial W_1^{[l]}} \right) \quad (11)$$

$$\frac{\partial J}{\partial b^{[l]}} = \frac{\partial J}{\partial z^{[l]}} \left(\frac{\partial z^{[l]}}{\partial b^{[l]}} + \frac{\partial z^{[l]}}{\partial h^{[l]}} \frac{\partial h^{[l]}}{\partial b^{[l]}} \right) \quad (12)$$

The changes in computation arise from the inclusion of the term h in the post-activation output computation, where h is computed using W_1 and b .

The procedure for computing the output layer gradients remains consistent with that of a conventional FNN.

2.7. Convergence Analysis

Upon analyzing the inference and learning mechanisms of CHNNNet, we found that it is expected to converge more rapidly than a conventional FNN.

To simplify the analysis, we assume that the bias b is a zero vector. Under this assumption, a conventional FNN employs a single learnable parameter W_1 , while CHNNNet employs two learnable parameters W_1 and W_2 . Consider the local loss function J_c associated with a hidden layer in CHNNNet and J_f associated with the corresponding hidden layer in a conventional FNN. At a given time step t of the learning process, J_c and J_f are formulated as follows:

$$J_c(W_1^t, W_2^t) = \|o^* - f(z_c^t)\| \quad (13)$$

$$J_f(W_1^t) = \|o^* - f(z_f^t)\| \quad (14)$$

In equation (13), z_c denotes the pre-activation output of a hidden layer of CHNNNet, while in equation (14), z_f denotes the pre-activation output of a hidden layer of a conventional FNN. In both equations, o^* represents the optimal output of the hidden layer that the learning mechanism aims to determine.

Following equation (1), the relation between z_c and z_f can be expressed as follows:

$$\begin{aligned} z_c &= z_f + W_2 h \\ &= z_f + W_2 z_f \\ &= (I + W_2) z_f \end{aligned} \quad (15)$$

To simplify the subsequent analysis, W_2 is assumed to be a zero matrix at time step $t-1$, which implies that z_c^{t-1} is equal to z_f^{t-1} . Thus, at time step $t-1$ the following holds:

$$\begin{aligned} \|o^* - f(z_c^{t-1})\| &= \|o^* - f(z_f^{t-1})\| \\ \Rightarrow J_c(W_1^{t-1}, W_2^{t-1}) &= J_f(W_1^{t-1}) \end{aligned} \quad (16)$$

In accordance with the convergence theorem of gradient descent, W_2 is updated to ensure that $f(z_c)$ approaches

o^* . Specifically, W_2 adjusts z_f such that the corresponding output $f(z_c)$ progressively approaches o^* , yielding predictions that are consistently closer to o^* than those produced by $f(z_f)$. Hence, at time step t , the following holds:

$$\begin{aligned} \|o^* - f(z_c^t)\| &< \|o^* - f(z_f^t)\| \\ \Rightarrow J_c(W_1^t, W_2^t) &< J_f(W_1^t) \end{aligned} \quad (17)$$

While the model has been analyzed using gradient-based methods, particularly backpropagation, equation (17) holds for any learning algorithm with theoretically guaranteed convergence.

Applying equation (16) in conjunction with inequality (17), we obtain the following:

$$J_c(W_1^{t-1}, W_2^{t-1}) - J_c(W_1^t, W_2^t) > J_f(W_1^{t-1}) - J_f(W_1^t) \quad (18)$$

Equation (18) indicates that the change in the loss of CHNNet between two successive time steps is greater than that of a conventional FNN. Consequently, CHNNet produces a steeper gradient, thus achieving faster convergence compared to conventional FNN.

3. Empirical Study

We empirically evaluated CHNNet on widely used architectures, including multilayer perceptrons (MLPs) and deep convolutional neural networks (CNNs). Since CHNNet inherently introduces additional parameters to implement intra-layer connections, we assessed its performance under equal-parameter conditions as well.

The models were trained using identical hyperparameters derived from the work of Kingma and Ba [11]. To ensure experimental fairness, all models were trained using identical weight initializations and fixed random seeds.

3.1. Experiment with MLP Architectures

We evaluated the convergence behavior of the CHNNet architecture in comparison to a conventional MLP architecture on the MNIST dataset. In the unequal parameter setting, the MLP comprised two fully connected layers with 1000 units each, resulting in 1.7 million parameters. In contrast, CHNNet, with two hidden layers of the same size but incorporating intra-layer connections, comprised 3.7 million parameters. As visualized in Figure 2(a), CHNNet exhibited a faster convergence than MLP within 200 epochs.

To ensure a balanced comparison, additional experiments were conducted with approximately equal parameter counts. In this setting, the MLP was widened to fully connected layers with 1,580 units each, resulting in roughly 3.7 million parameters, closely matching the 3.7 million parameters of CHNNet. Despite achieving near parity in parameter count, CHNNet consistently demonstrated faster convergence, as illustrated in Figure 2(b).

In both experiments, we used a learning rate of 1×10^{-3} , batch size of 128, and sparse categorical crossentropy loss with logits disabled. ReLU nonlinearities activated the hidden layers, with softmax applied at the output to produce class probabilities for the 10-class classification task. This consistent training regimen, implemented in TensorFlow, facilitated a controlled and rigorous comparison of the models on MNIST.

3.2. Experiment with CNN Architectures

3.2.1. Convolutional Adaptation of CHNNet

Consider that $x \in \mathbb{R}^{h \times w \times c_{in}}$ denotes the input feature map, where h and w represent the height and width of the input feature map and c_{in} is the number of input channels. For the l^{th} layer, the model first computes an intermediate feature map as follows:

$$h_i^{[l]} = x^{[l]} * K_i^{[l]}; K_i^{[l]} \in \mathbb{R}^{k_h^{[l]} \times k_w^{[l]} \times c_{in}^{[l]} \times c_{out}^{[l]}} \quad (19)$$

Here, k_h and k_w represent the height and width of the kernel, while c_{in} and c_{out} denote the number of input and output channels, respectively. In fact, equation (19) corresponds to the identity mapping as described in equation (2). Subsequently, The model computes the following:

$$h_h^{[l]} = h_i^{[l]} * K_h^{[l]}; K_h^{[l]} \in \mathbb{R}^{\tilde{k}_h^{[l]} \times \tilde{k}_w^{[l]} \times c_{out}^{[l]} \times c_{out}^{[l]}} \quad (20)$$

When the spatial kernels are shared across channels, \tilde{k}_h and \tilde{k}_w are equal to k_h and k_w , respectively. Conversely, when kernel sharing is not applied, \tilde{k}_h and \tilde{k}_w are equal to 1.

Subsequently, the pre-activation output is computed as follows:

$$z^{[l]} = h_i^{[l]} + h_h^{[l]} \quad (21)$$

This formulation aligns with the pre-activation computation for hidden layers in equation (1) under the identification $a^{[l-1]} \equiv x^{[l]}$, $h^{[l]} \equiv h_i^{[l]}$, $W_1^{[l]} \leftrightarrow K_i^{[l]}$, $W_2^{[l]} \leftrightarrow K_h^{[l]}$, and $b^{[l]} = \vec{0}$.

In the linear case with unit hidden stride, the composition reduces to a single effective kernel $K_e = K_i + (K_i * K_h)$. This is consistent with the one-layer reduction presented in equation (8) and emphasizes that the intra-layer term of CHNNet represents a same-step coupling.

3.2.2. Experiments

We evaluated the convergence behavior of CHNNet against a conventional CNN architecture on CIFAR-10. In the unequal-parameter setting, both models consisted of three stacked convolutional stages with 5×5 kernels and same padding, featuring channel widths of 64, 128 and 256. Each stage is followed by batch normalization, a rectified linear unit activation, and a 3×3 max pooling with stride

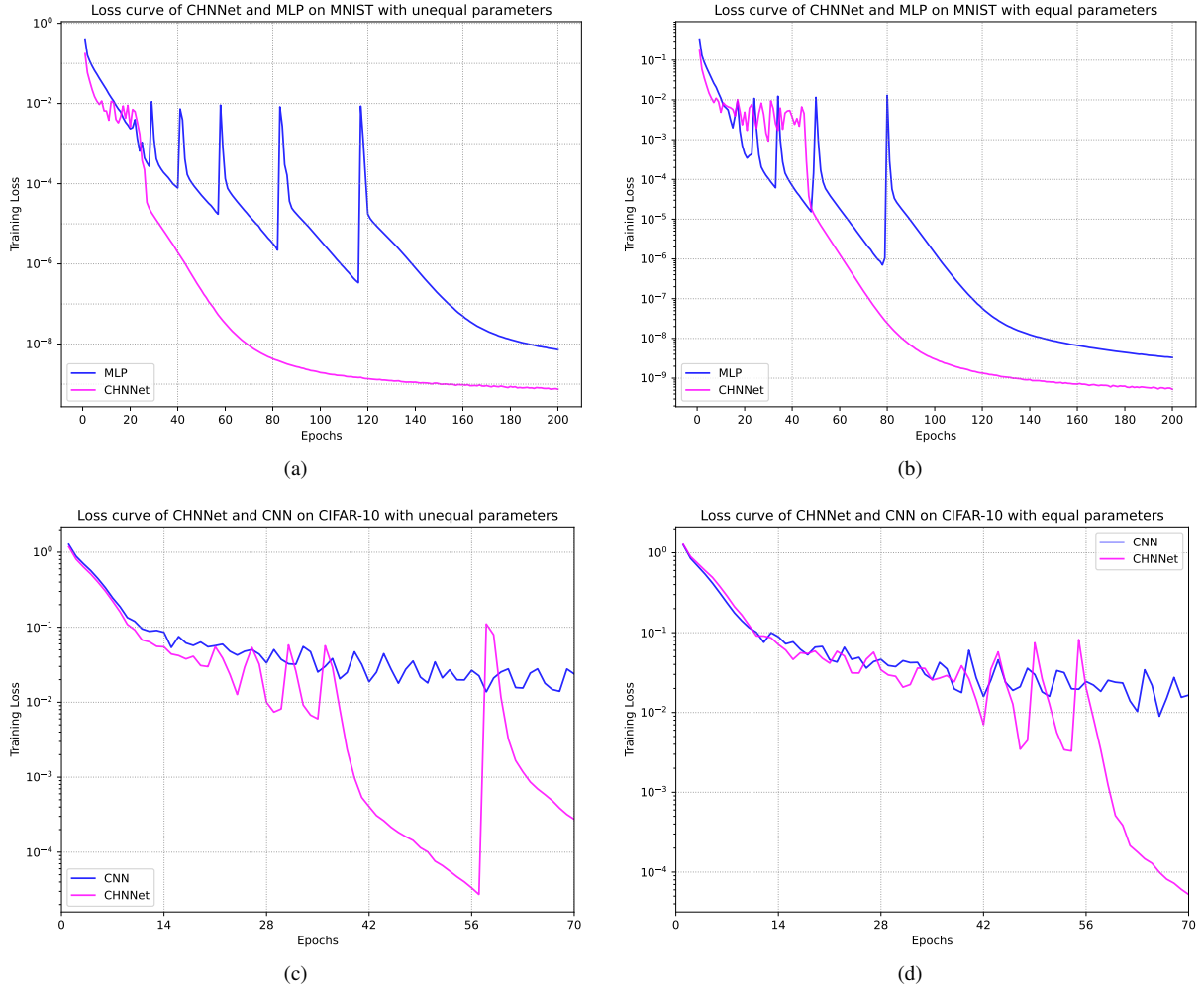


Figure 2. Loss curves on (a–b) MNIST and (c–d) CIFAR-10 datasets. (a) MLP and CHNNet with unequal parameters, (b) MLP and CHNNet with equal parameters, (c) CNN and CHNNet with unequal parameters, (d) CNN and CHNNet with equal parameters.

2 and valid padding. The classifier head flattened the feature representation and applied a fully connected layer with 1000 units, followed by batch normalization, rectified linear activation, and 10-way softmax output. The baseline CNN comprised 3.3 million parameters, whereas the CHN-Net variant, which introduces intra-layer channel mixing at each stage while maintaining the same depth and pooling structure, contained 4.4 million parameters. The loss curve of CHNNet in Figure 2(c) show an overall downward trend, with a transient spike around epoch 55 before resuming their decline. This behavior is presumably due to moment-based update volatility on an atypical mini-batch interacting with batch normalization updates late in training, temporarily perturbing the running statistics before they realign.

To provide a balanced comparison, we also conducted experiments with a matched number of parameters. The conventional CNN was widened to 90, 150 and 280 chan-

nels followed by a fully connected head with 1250 units, resulting in 4.5 million parameters, whereas CHNNet retained 64, 128 and 256 channels with a 1000-unit CHN head. Despite this near parity, CHNNet retains its convergence advantage, as visualized in Figure 2(d).

In the experiments, the inputs were standardized per channel and the models were trained using mini-batches of size 128 and the Adam optimizer with $\beta_1 = 0.9$, $\beta_2 = 0.999$, and $\varepsilon = 10^{-8}$ at a learning rate of 1×10^{-4} . Both the unequal-parameter and matched-parameter experiments were run for 70 epochs under the same training schedule and evaluation settings.

3.3. Discussion

CHNNet consistently outperformed the baseline architectures in both fully connected and convolutional settings, as illustrated in Figure 2. As reported in Table 1, CHN-

Table 1. Comparison of MLP and CHNNet.

Model	Total Params	Accuracy	Loss
MLP	1.7M	0.9836	0.1509
CHNNet	3.7M	0.9860	0.1208
MLP	3.7M	0.9847	0.1309
CHNNet	3.7M	0.9870	0.1163

Table 2. Comparison of CNN and CHNNet.

Model	Total Params	Accuracy	Loss
CNN	3.3M	0.7122	2.2610
CHNNet	4.4M	0.7941	1.0325
CNN	4.5M	0.7452	1.9401
CHNNet	4.4M	0.7747	1.1329

Net achieved slightly higher test accuracy and lower loss than the MLP, demonstrating the effectiveness of its intra-layer connection mechanism. Similarly, Table 2 shows that CHNNet surpassed the CNN in accuracy while exhibiting reduced loss, indicating that intra-layer mixing strengthens convolutional feature extraction.

Evaluation under equal-parameter configurations provides additional insight into the source of these improvements. In both MLP and CNN settings with increased parameters, CHNNet converged more rapidly and consistently attained higher accuracy with lower loss than the baseline models. These results suggest that the performance gains stem primarily from the architectural advantages introduced by intra-layer connections, rather than from the differences in parameter count.

4. Future Work

While CHNNet demonstrates the potential benefits of incorporating intra-layer connectivity in feedforward networks, several promising directions merit further study:

- While CHNNet presents one approach to intra-layer connectivity, exploring alternative patterns or weighting strategies for hidden neuron interactions may uncover more efficient or stable configurations that further enhance the performance of the network.
- CHNNet has thus far been evaluated within the MLP and CNN architectures. However, its applicability could be further examined across other paradigms such as Recurrent Neural Networks (RNNs), Spiking Neural Networks (SNNs), Variational Autoencoders (VAEs), and Transformers, where introducing intra-layer connectivity may have significant implications for learning dynamics.
- CHNNet has so far been evaluated exclusively using the backpropagation algorithm. Its compatibility and per-

formance with alternative learning methods, such as the forward-forward algorithm [6] or predictive coding [17], remain to be explored.

- The effects of hyperparameters such as activation functions, optimization algorithms, and other training configurations on CHNNet’s performance are yet to be rigorously studied.

5. Conclusion

In this study, we investigate the impact of introducing intra-layer connectivity among hidden neurons within conventional feedforward architectures. The principal contributions of this work are summarized as follows:

- We introduce CHNNet, a biologically plausible network with intra-layer connections among hidden neurons, facilitating efficient information sharing within each hidden layer.
- We formulate equations for hidden layer activations for the inference process and adapt the backpropagation algorithm to compute gradients accordingly during the learning process.
- Through theoretical analysis of the model, we demonstrate that CHNNet achieves faster convergence compared to conventional FNNs.
- We have evaluated the proposed model on benchmark datasets and empirically demonstrated a substantial improvement in convergence rate compared to conventional FNNs.

The study underscores that even minimal structural modifications, specifically introducing interactions among hidden neurons, can enhance the learning behavior of standard architectures. This work points toward a broader reconsideration of connectivity patterns in neural networks, suggesting that gains in efficiency and stability may arise not only from increased depth or complexity, but also from fostering richer intra-layer coordination.

References

- [1] Long Chen, Xuhang Li, Yaqin Zhu, Haitao Wang, Jiayong Li, Yu Liu, and Zijian Wang. Intralayer-connected spiking neural network with hybrid training using backpropagation and probabilistic spike-timing dependent plasticity. *International Journal of Intelligent Systems*, 2023(1):3135668, 2023. [1](#), [2](#)
- [2] Xiang Cheng, Yunzhe Hao, Jiaming Xu, and Bo Xu. Lisnn: Improving spiking neural networks with lateral interactions for robust object recognition. In *Proceedings of the Twenty-Ninth International Joint Conference on Artificial Intelligence, IJCAI-20*, pages 1519–1525. International Joint Conferences on Artificial Intelligence Organization, 2020. Main track. [1](#), [2](#)
- [3] Francis Crick and Edward Jones. Backwardness of human neuroanatomy. *Nature*, 361(6408):109–110, 1993. [1](#)

[4] Stephen Grossberg. Competitive learning: From interactive activation to adaptive resonance. *Cognitive Science*, 11(1):23–63, 1987. [1](#)

[5] Kaiming He, Xiangyu Zhang, Shaoqing Ren, and Jian Sun. Deep residual learning for image recognition. *IEEE Conference on Computer Vision and Pattern Recognition (CVPR)*, pages 770–778, 2016. [1, 3](#)

[6] Geoffrey Hinton. The forward-forward algorithm: Some preliminary investigations, 2022. [6](#)

[7] G. Hinton and Terrence Sejnowski. Learning and relearning in boltzmann machines. *Parallel Distributed Processing*, 1, 1986. [2](#)

[8] John Hopfield. Neural networks and physical systems with emergent collective computational abilities. *Proceedings of the National Academy of Sciences of the United States of America*, 79:2554–2558, 1982. [2](#)

[9] Gao Huang, Zhuang Liu, Laurens Van Der Maaten, and Kilian Q. Weinberger. Densely connected convolutional networks. *IEEE Conference on Computer Vision and Pattern Recognition (CVPR)*, pages 2261–2269, 2017. [3](#)

[10] Herbert Jaeger. The “echo state” approach to analysing and training recurrent neural networks-with an erratum note’. *Bonn, Germany: German National Research Center for Information Technology GMD Technical Report*, 148, 2001. [2](#)

[11] Diederik P. Kingma and Jimmy Ba. Adam: A method for stochastic optimization, 2017. [4](#)

[12] Thomas N. Kipf and Max Welling. Semi-supervised classification with graph convolutional networks, 2017. [1](#)

[13] Jia Liu, Maoguo Gong, Liang Xiao, Wenhua Zhang, and Fang Liu. Evolving connections in group of neurons for robust learning. *IEEE Transactions on Cybernetics*, 52(5):3069–3082, 2022. [1](#)

[14] Wolfgang Maass, Thomas Natschläger, and Henry Markram. Real-time computing without stable states: A new framework for neural computation based on perturbations. *Neural computation*, 14:2531–2560, 2002. [2](#)

[15] Warren S. McCulloch and Walter Pitts. A logical calculus of the ideas immanent in nervous activity. *Bulletin of Mathematical Biophysics*, 5(4):115–133, 1943. [1](#)

[16] Marvin Minsky and Seymour Papert. *Perceptrons: An Introduction to Computational Geometry*. MIT Press, Cambridge, MA, USA, 1969. [2](#)

[17] R. P. N. Rao and D. H. Ballard. Predictive coding in the visual cortex: A functional interpretation of some extra-classical receptive-field effects. *Nature Neuroscience*, 2(1):79–87, 1999. [6](#)

[18] Olaf Ronneberger, Philipp Fischer, and Thomas Brox. U-net: Convolutional networks for biomedical image segmentation. In *Medical Image Computing and Computer-Assisted Intervention – MICCAI 2015*, pages 234–241, Cham, 2015. Springer International Publishing. [3](#)

[19] D. E. Rumelhart, G. E. Hinton, and R. J. Williams. Learning internal representations by error propagation. *Parallel Distributed Processing: Explorations in the Microstructure of Cognition, Vol. 1: Foundations*, page 318–362, 1986. [2](#)

[20] Shao-Qun Zhang and Zhi-Hua Zhou. Theoretically provable spiking neural networks. *Advances in Neural Information Processing Systems*, 35:19345–19356, 2022. [1, 2](#)

[21] Shao-Qun Zhang, Zhao-Yu Zhang, and Zhi-Hua Zhou. Bifurcation spiking neural network. *Journal of Machine Learning Research*, 22(253):1–21, 2021. [1, 2](#)

[22] Zongwei Zhou, Md Mahfuzur Rahman Siddiquee, Nima Tajbakhsh, and Jianming Liang. Unet++: A nested u-net architecture for medical image segmentation. *Deep Learning in Medical Image Analysis and Multimodal Learning for Clinical Decision Support*, pages 3–11, 2018. [3](#)